

Turbulence measurements with μ -PIV in large-scale pipe flow

by

R. Lindken⁽¹⁾, F. Di Silvestro⁽²⁾, J. Westerweel⁽¹⁾ and F.T.M. Nieuwstadt⁽¹⁾

⁽¹⁾Laboratory of Aero- and Hydrodynamics,
J.M. Burgerscenter
Delft University of Technology,
Leeghwaterstraat 21, 2628 CA Delft; The Netherlands
www.ahd.tudelft.nl; E-Mail: r.lindken@wbmt.tudelft.nl

⁽²⁾Universita degli Studi di Roma "La Sapienza"
Facolta di Ingegneria Aerospaziale

ABSTRACT

A microscopic Particle Image Velocimetry (μ -PIV) system for measurements in a large scale wind tunnel has been developed. The working distance of the μ -PIV system is 550 mm with a magnification factor of 2.6.

The long distance μ -PIV system is a combination of a conventional PIV system with light-sheet illumination and a μ -PIV system with volume illumination. For the evaluation of the velocity data an iterative PIV cross-correlation algorithm is used. The performance of the measurement technique depends on the particle density in an interrogation volume, which has a depth in the range of 200 μm . For that reason we used a high load of tracer particles with a size of 380 nm. The smallest size of the interrogation window was 32 x 32 px at which an unreasonably high number of outliers was found (65 % good vectors at 21 μm resolution). With an interrogation field size of 64 x 64 px the number of good vectors increased to more than 80 % at 42 μm resolution.

The measurement device is tested in turbulent pipe flow at $Re = 15300$. Fig 1. shows an overview of the results. The resolution of the velocity data is 42 μm . The smallest structures in turbulent pipe flow are expected in the range of 5 times the Kolmogorov scale, which is in the range 40 μm . The size of the flow structure in Fig. 1 is about 200 μm .

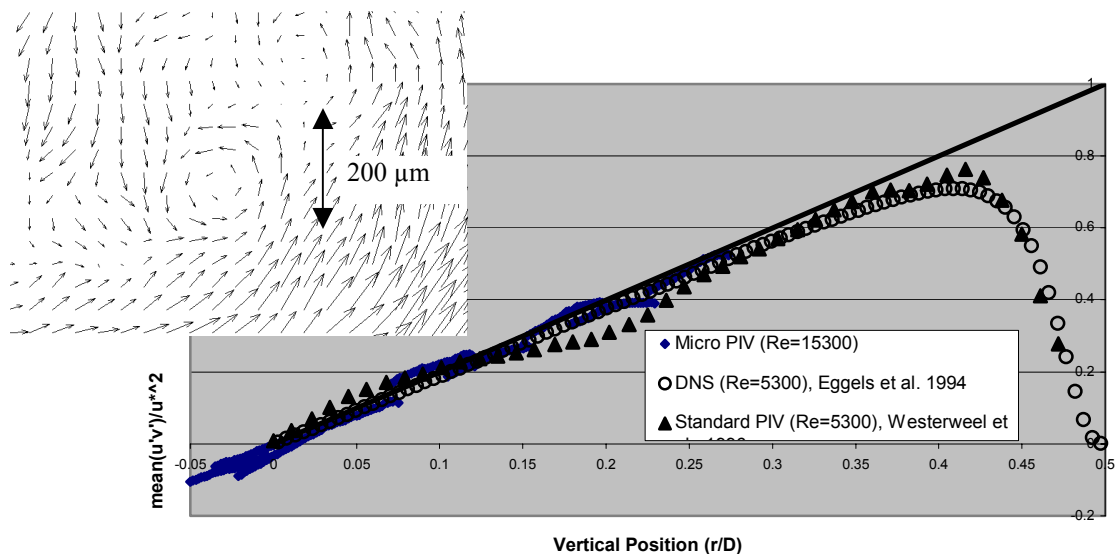


Fig. 1.: Test result of turbulent pipe flow at $Re = 15300$: A vortical structure with the size of 5 times the Kolmogorov scale (left) and the Reynolds stress profile for turbulent pipe flow (right).

1. INTRODUCTION

In most technological and industrial applications the flow is characterized by a Reynolds number that is much higher than the Reynolds number that can be reached in standard laboratory experiments. As a result current turbulence models cannot be tested under high Re number flow conditions. For that purpose we plan to construct a high pressure wind tunnel in which turbulent flow experiments at high Reynolds number are possible. Our aim is to reach a Reynolds number (based on the macro length and velocity scale of turbulence) of the order of 10^5 . The most important obstacle to perform turbulence measurements at very high Reynolds number in such facility is that the micro-scales of turbulence will become very small indeed. This follows directly from the relationship

$$\eta = l \text{Re}^{-\frac{3}{4}},$$

which for the Reynolds number mentioned above and $l \approx 0.05$ m leads to $\eta \approx 5 \mu\text{m}$.

Furthermore, if one wants to sample all flow scales simultaneously, i.e. from the macro- to the micro-scale, an area of the size of the largest scale has to be observed with the resolution of the smallest scale. The ratio of the largest to the smallest resolvable scale is called the spatial dynamic range (SDR) and from the ration of the macro- to micro length scale given above it follows that

$$SDR = \frac{l}{\eta} \sim \text{Re}^{\frac{3}{4}}$$

The SDR value determines the highest ‘effective’ Reynolds number that can be fully resolved. For the aforementioned Reynolds number $\text{Re} \approx 10^5$, the SDR must be equal to ~ 10000 .

The ratio of the highest and the lowest velocity that has to be resolved in one measurement is called the velocity dynamic range VDR. For a mean flow of 1 m/s and a turbulence intensity of 1 % the VDR becomes equal to 100 with smallest velocities to be resolved in the order of 10 mm/s.

It will be clear that theses requirements on the SDR, VDR and resolution will pose strong demands on a measurement system.

Table 1: Requirements for turbulence measurements in a high pressure wind tunnel

Spatial Dynamic Range (SDR)	$\frac{l}{\eta} \sim \text{Re}^{\frac{3}{4}}$	Very high to fully resolve high Reynolds-numbers
Spatial resolution of the measurement volume	$\Delta x \approx 5 \cdot \eta$	Very high to resolve smallest flow scales
Velocity Dynamic Range (VDR)	$\frac{u'}{U_m} \sim 1\% - 10\%;$ $\frac{u'_{macro}}{u'_{micro}} \sim \text{Re}^{\frac{1}{4}}$	High, because of low turbulence intensity (1-10 %)

2. EXPERIMENTAL SET-UP

2.1 Measurement Technique

We have chosen Micro Particle Image Velocimetry (μ -PIV) as a measurement technique. To demonstrate that measurements, which satisfy above requirements, are feasible, a pilot project has been carried out.

Comparable measurement devices have been used by Urushihara et al. (1993) and Dieterle (1997). In our case we use a μ -PIV system with an extremely large working distance of 0.55 to 1.3 m, which is needed to avoid flow disturbance for the future application in the wind tunnel. The μ -PIV system consists of a frequency-doubled Nd:YAG laser operated at 130 mJ / pulse, a 1k x 1.3k double shutter CCD-camera and a long distance microscope. We have chosen a Questar QM-1 long distance microscope with at the minimum working distance of 550 mm.

Extra effort is necessary for guiding the laser light to the measuring area and to realize a high seeding quality. Particles in various sizes from 200 nm to 1.5 μ m have been tested. Based on these tests we have chosen stabilized fluorescent silica particles with a nominal diameter of 380 nm (Verhaegh and Van Blaaderen, 1994).

In order to evaluate the recordings with a high accuracy enough tracer particles have to be in the measurement volume. Unlike in stationary flows in microscopic channels we cannot use ensemble averaging (Meinhart et al., 2000) for the μ -PIV evaluation. Ensemble averaging of 8 pictures would result in a time average of 1.0 sec, which is several orders higher than the Kolmogorov time scale for turbulent flows in which we aim to measure. First measurements with a long distance microscope with a depth of field of about 200 μ m showed that the limiting factor for a successful PIV measurement is the number of particles in the three-dimensional measurement volume. Therefore we decided to use tracer particles of 380 nm in diameter, in order to achieve a very high particle density without a high volume fraction of tracer particles.

Figure 2 shows the illumination principle in standard PIV compared to μ -PIV. For PIV a quasi-two-dimensional light sheet illuminates the tracer particles. The depth of the measurement volume Δz_0 is defined by the thickness of the light sheet Δz . The depth of focus of the photo lens is much larger than the thickness of the light sheet. Whereas for μ -PIV volume illumination is used (Meinhart et al 1999, 2000). The depth of focus of the optical system Δz therefore defines the depth of the measurement volume Δz_0 . The disadvantage of the volume illumination set-up is the appearance of out of focus particles, which appear blurred in the image (Wereley et al, 2000). For μ -PIV using microscope lenses the very sharp edge of the focus plane partly compensates the negative effect of out-of-focus particles. With the help of image processing the remaining blurred images of particles that have a much lower intensity than in-focus particles, are in that case removed from the PIV-recordings.

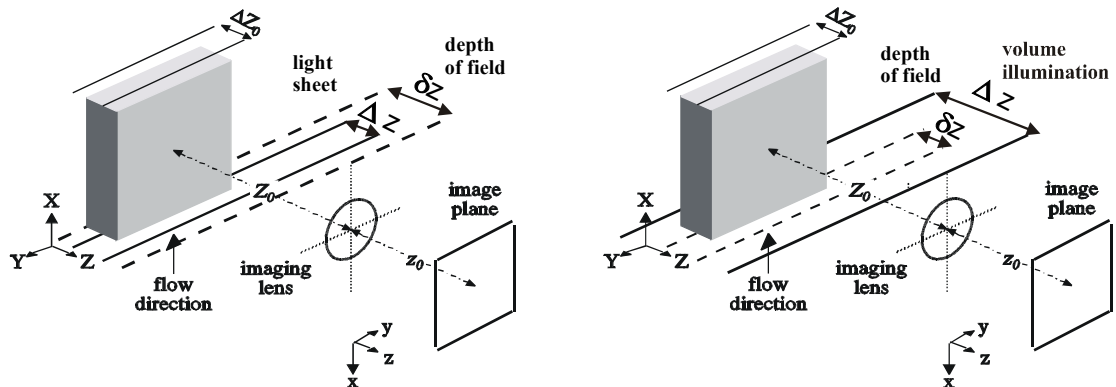


Fig. 2.: The illumination set-up for standard PIV (left) compared to μ -PIV (right)

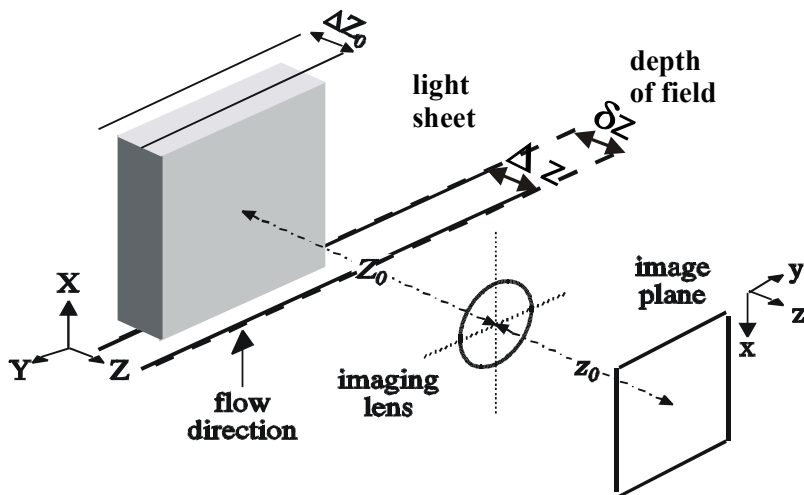


Fig. 3.: The illumination set-up for μ -PIV applied a set-up with a long-distance microscope.

The long distance microscope which we use for our μ -PIV measurements does not have a sharp edge of the focal plane. For that reason out-of-focus particles have the same intensity as in-focus particles and as a result they form an important error source. We solve this problem with an optimized illumination set-up in figure 3. In this set-up the depth of focus of the long distance microscope δz and the thickness of the light sheet Δz are the same size so that out of focus particles are no longer illuminated and no longer lead to noise in our images. The disadvantage of this method is, that the two laser light sheets have to overlap perfectly. The accuracy of the overlap of the two laser light sheets has to be better than $20 \mu\text{m}$, which is about 10% of the light sheet depth of $200 \mu\text{m}$.

Such an accurate overlap is achieved with the use of height of the peak of the cross-correlation-function as an indicator of the overlap of the two light sheets.

Another effect of this special illumination set-up for μ -PIV is the influence of the polarization direction on the scattering behavior of small particles (particle diameter $d_p < \lambda$). Fig. 4 taken from Born and Wolf (1975) presents measurements carried out by Blumer (1926) which illustrate that the for polarized light (e.g. from a Nd:YAG laser) the particle scattering cross-section for small particles depends on the polarization direction.

Table 2 gives an overview over the differences between μ -PIV and long distance μ -PIV

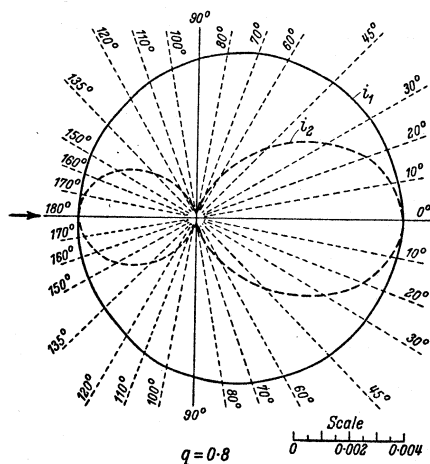


Fig. 4.: The scattering behavior of small particles ($d_p < \lambda$) for polarized light (from Born and Wolf, 1975). Polarized light illuminating a particle from the left (small arrow) is reflected at different intensities of the two orthogonal polarization directions (permanent and dotted lines). This effect depends on the scattering angle. It is maximum at 90° and minimum at 0° and 180° .

Table 2: Differences in image acquisition between μ -PIV and long distance μ -PIV

Working distance	0 – 30 mm	550 – 1300 mm
Illumination	Volume	Light sheet
Mode	$\delta z < \Delta z_0$	$\delta z \approx \Delta z_0$
Scattering angle	$0^\circ, 180^\circ$	90°
Polarization	Not important	Important

2.2 Flow Facility

As mentioned above the experiment serves as a pilot project to prove the feasibility of turbulence measurements in a high Reynolds number flow facility. We have chosen to carry out our test experiment with a turbulent pipe flow in a closed loop water facility. A frequency-controlled pump is used to set the flow rate. The test section, where the measurements are carried out, consists of a smooth pipe with an inner diameter of 50 mm. At the inlet of the straight pipe the flow is triggered to turbulence by a flow disturber. The flow is expected to be fully developed at the test section, which is mounted 80 diameters downstream of the inlet. The measurement section consists of very thin glass pipe (2.0 mm thickness of the walls) with the same inner diameter of 50 mm as the rest of the pipe. The thin pipe is surrounded by a square, water filled box, in order to minimize optical distortions due to curved pipe surfaces.

The maximum flow velocity that could be achieved in this facility is 0.3 m/s, which is equivalent to $Re = 15300$ based on the diameter and the mean velocity. Higher flow velocities are possible, but in that case we found that the onset of cavitation in the pump generates micro bubbles in the flow. These micro bubbles would disturb the measurements.

3. MEASUREMENTS

With the μ -PIV set-up we measured the velocity profile in the upper half of the pipe. The flow was measured in the center region of the pipe only. In this region reflections did not disturb the measurements. Due to the low particle density and as a consequence the low signal measurements in the wall region of the flow were strongly disturbed by the high noise level from reflections at the curved wall. The region of interrogation for one set of measurements is $3.3 \times 2.6 \text{ mm}^2$. By traversing the camera together with the long-distance microscope we measured the velocity distribution at 7 positions from $r/D = 0$ to $r/D = 0.3$ from the center of the pipe.

The PIV-measurements are evaluated with standard cross-correlation methods. Each image frame is interrogated in 32×32 - pixel sub images with an overlap of 50% corresponding to intervals of 16 pixels. With a scale factor of 383 px/mm the corresponding width of the measurement region is $41 \mu\text{m}$. The information density (vector spacing) is $20 \mu\text{m}$.

Urushihara et al. (1993) explain that due to the low particle image density in their PIV measurements with a macro lens, they could only evaluate 70 % good vectors with a interrogation field of $128 \times 92 \text{ px}$. In our case for the evaluation with a $32 \times 32 \text{ px}$ interrogation field we evaluated only 65 % good vectors. For that reason the evaluation has been redone with an interrogation field of $64 \times 64 \text{ px}$. In that case 80 % good vectors were obtained. The resolution is $82 \mu\text{m}$ for the width of the measurement area. The information density (vector spacing) is $41 \mu\text{m}$.

Figures 5 to 8 present examples of flow structures observed at the center of the pipe. In all vector plots we present the instantaneous velocity distribution relative to the average convection velocity of the individual measurement. The convection velocity of an individual measurement is different from the convection velocity of all measurements, which is $U_c = 0.301 \text{ m/s}$. The Kolmogorov length scale is about $40 \mu\text{m}$.

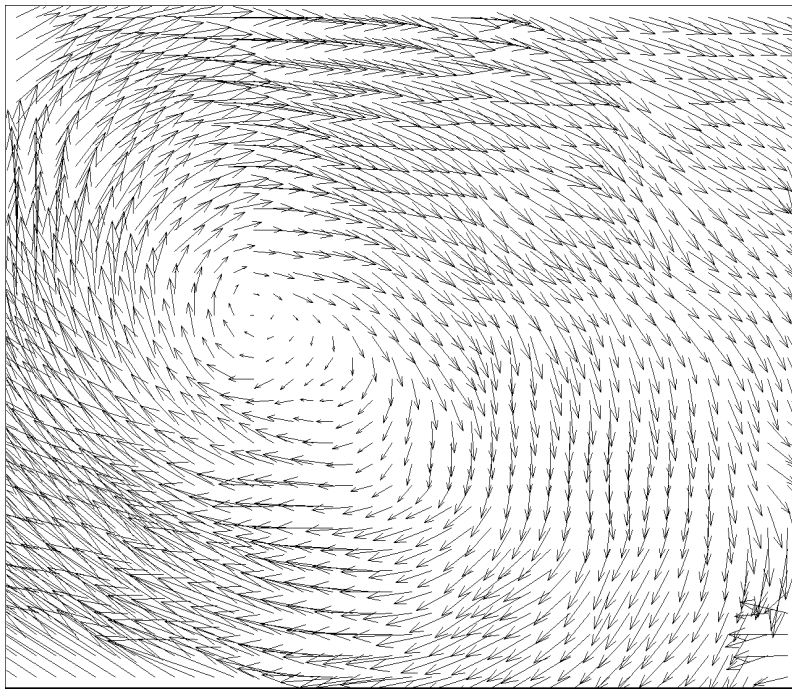


Fig. 5.: A typical instantaneous flow structure in the center of the pipe. The vector plot represents the velocity distribution relative to the mean velocity of all data in this vector plot. This mean velocity is 20 times larger than the largest vector of the relative velocities. The vector plot shows a large vortical structure with dimensions larger than the field of view ($3.3 \times 2.6 \text{ mm}^2$).

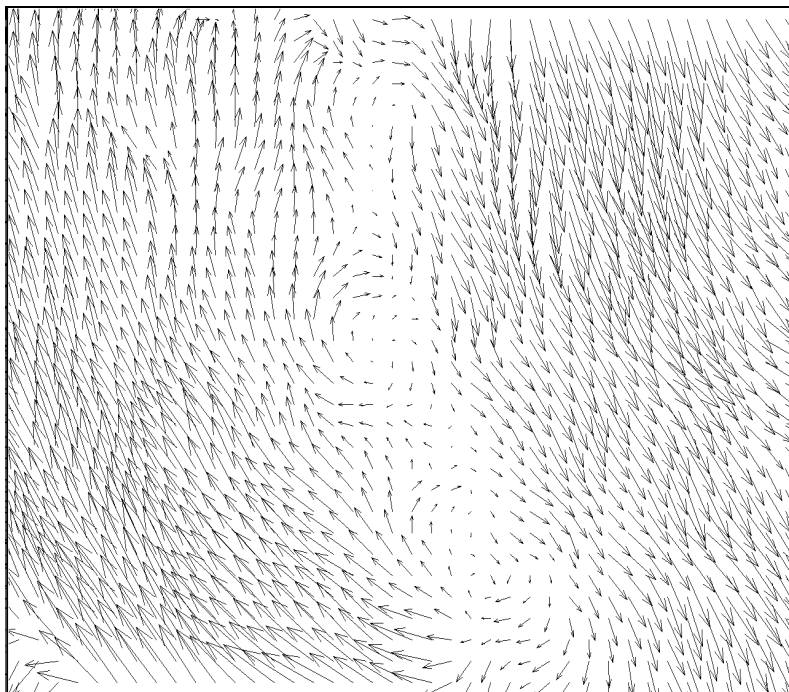


Fig. 6.: Another example of a typical instantaneous flow structure in the center of the pipe. For information about the vectors shown we refer to figure 5. The vector plot shows high shear, which seems to coincide with numerous small vortices.

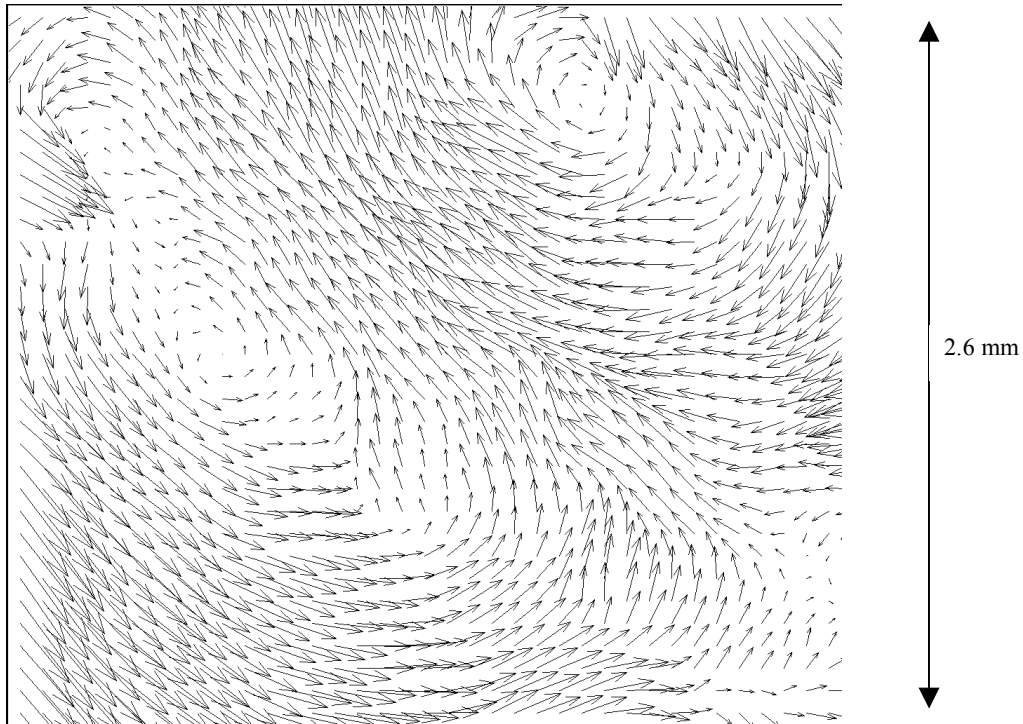


Fig. 7.: A rare instantaneous flow structure in the center of the pipe. For information about the vectors shown we refer to figure 5. Two counterrotating vortices are recorded in this measurement.

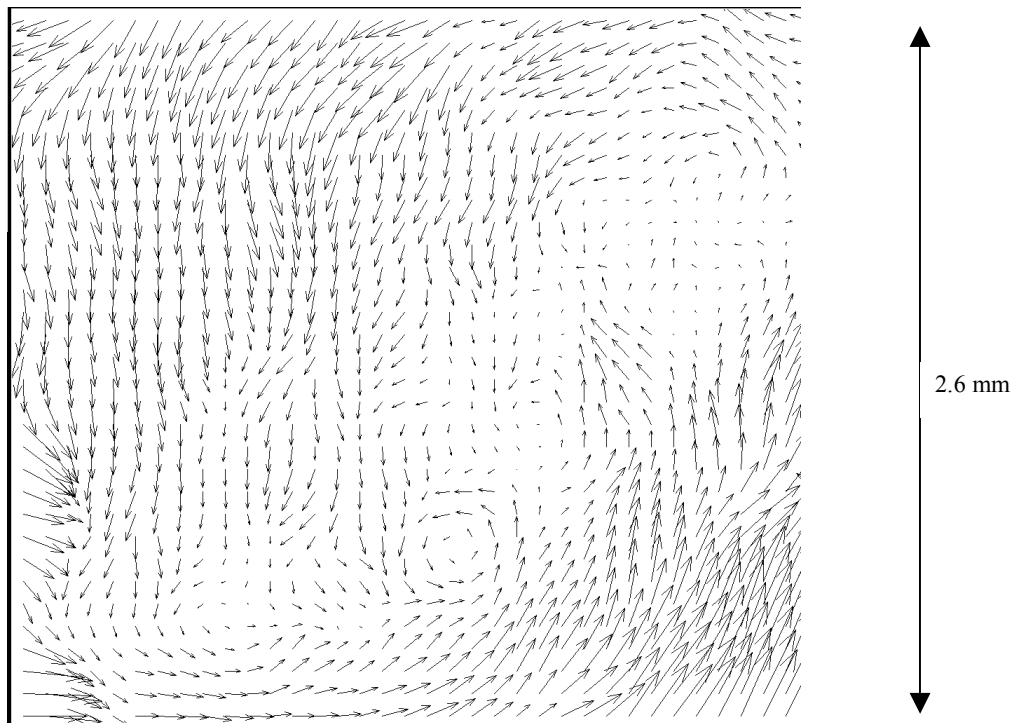


Fig. 8.: A rare instantaneous flow structure in the center of the pipe. For information about the vectors shown we refer to figure 5. In the lower part of the vector plot a small vortex can be seen. The size of the vortical structure is about 5 times the Kolmogorov scale.

The most common flow structures are large vortices (Fig. 5) and regions of high shear with numerous small vectors in the high shear region (Fig. 6). Figures 7 and 8 present some rare events that we captured. Fig. 7 shows a counterrotating pair of vortices, while in Fig. 8 a small vortex is recorded. The dimensions of the vortex shown are about $200 \times 280 \mu\text{m}^2$, which corresponds to 5 times the Kolmogorov scale. The vortex has the size of the smallest expected structure in the flow.

4. RESULTS

The mean profile for the velocity component U in main flow direction and the component in radial direction V are presented in Fig. 9. Each mean velocity data point consists of 1000 statistically independent PIV-measurements.

The measurements of the velocity U in the main flow direction give a good representation of the turbulent velocity profile at $\text{Re} = 15300$. The measurement of the velocity V , which shows that this component is zero (0.05 px), indicates a negligible misalignment.

In Figs. 10 and 11 we show the r.m.s. values of the axial and radial velocity fluctuations normalized with the friction velocity u_* as described in Westerweel et al. (1993).

As reference the results of the DNS computation by Eggels et al. (1994) and PIV measurements by Westerweel et al. (1996) are plotted in the same figure.

The measured turbulence data follow the reference DNS data very well. The velocity fluctuations in the main flow direction are in the same range. The velocity fluctuations in the axial direction are slightly higher than the DNS data.

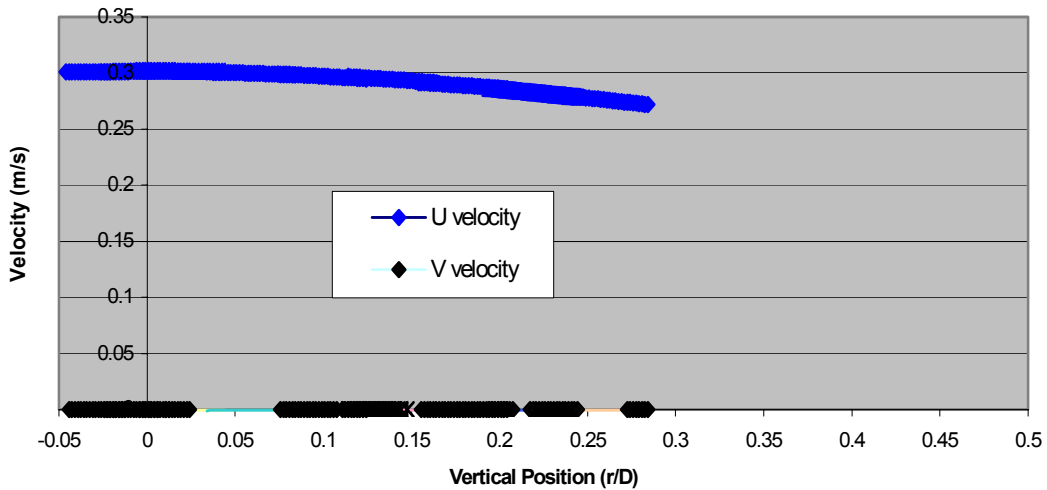


Fig. 9.: The velocity profile in the main flow direction (U velocity) and the velocity in the radial direction (V velocity) as a function of the dimensionless distance r/D from the centerline.

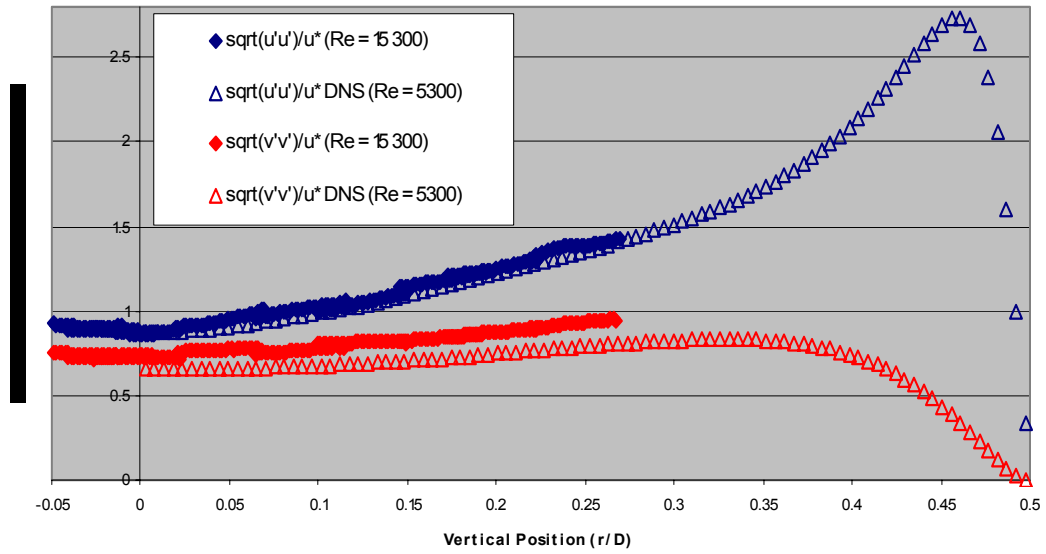


Fig. 10.: The profile of the axial and radial turbulence intensities (u' and v' respectively), normalized by the friction velocity as a function of the dimensionless distance r/D from the centerline.

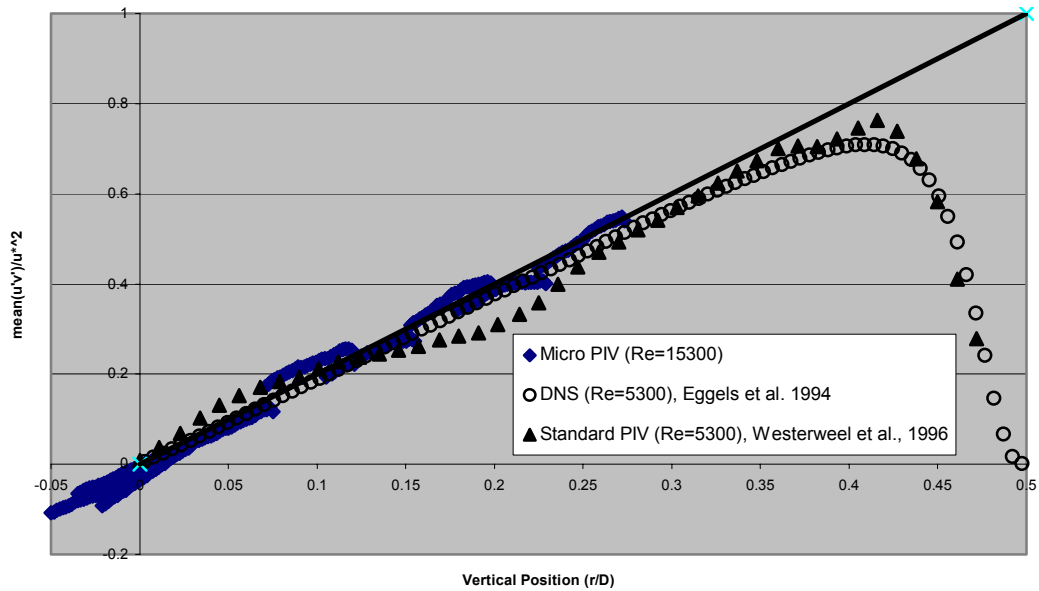


Fig. 11.: The profile of the Reynolds stress $\langle u'v' \rangle$, normalized by the friction velocity as a function of the dimensionless distance r/D from the centerline.

5. CONCLUSIONS

We have successfully measured turbulence in fully developed turbulent pipe flow at $Re = 15300$ with a long distance microscope. The experimental quality of the profiles of the velocity fluctuations and the Reynolds stress prove the ability of the long distance μ -PIV system to measure turbulence at high Reynolds-number. Based on the measurements system we have visualized the smallest turbulent structures sized 5 times the Kolmogorov scales. The size of the smallest scales is about $200\mu\text{m}$. We need 3×3 vectors to resolve a vortical structure. With a resolution of the μ -PIV system of $21\mu\text{m}$ we would be able to measure structures of size $63 \times 63\mu\text{m}^2$.

The resolution of the system can be further improved by the use of a customized long distance microscope, improvement in seeding and the application of adapted evaluation algorithms.

ACKNOWLEDGEMENT

We would like to thank Ron Adrian, University of Illinois, for making suggestions at an early stage of this research project.

This research was funded by the Foundation for Fundamental Research on Matter (FOM)

REFERENCES

- Born, M. and Wolf, E. (1975): "Principles of Optics", Pergamon Press, Oxford, Great Britain.
- Blumer, H. (1925): Zeitschrift für Physik, 32, pp. 119ff.
- Dieterle, L. (1997): „Entwicklung eines abbildenden Meßverfahrens (PIV) zur Untersuchung von Mikrostrukturen in turbulenten Strömungen.“ PhD-Thesis, Deutscher Universitätsverlag, Wiesbaden, Germany.
- Eggels, J.G.M. Unger, F. Weiss, M.H. Westerweel, J. Adrian, R.J. Friedrich, R. Nieuwstadt, F.T.M. (1994): "Fully turbulent pipe flow: A comparison between direct numerical simulation and experiment." Journal of Fluid Mechanics, 268, pp.175-209.
- Meinhart, C.D. Wereley, S.T. Santiago, J.G. (1999): "PIV measurements of a microchannel flow." Experiments in Fluids 27, pp. 414-419.
- Meinhart, C.D. Wereley, S.T. Santiago, J.G. (2000): "Micron Resolution Velocimetry Techniques." Laser Techniques applied to fluid mechanics: Selected papers from the 9th Int. Symp, Lisbon, Springer, Berlin, Germany, pp. 57-70.
- Meinhart, C.D. Wereley, S.T. Santiago, J.G. (2000): "A PIV Algorithm For Estimating Time-Averaged Velocity Fields." Journal of Fluids Engineering 122, pp. 285-289.
- Urushihara, T. Meinhart, C.D. and Adrian, R.J. (1993): "Investigation of the logarithmic layer in pipe flow using particle image Velocimetry." Near Wall Turbulence Flows, Elsevier, Amsterdam, The Netherlands, pp 433-446.
- Verhaegh, N.A.M. and Van Blaaderen, A. (1994): "Dispersions of rhodamine-labeled silica spheres: synthesis, characterization, and fluorescence confocal scanning laser microscopy." Langmuir 10, pp. 1427-1438.
- Wereley, S.T. Meinhart, C.D. and Gray m.H.B. (2000): "Depth effects in volume illuminated Particle Image Velocimetry." Proc. of the 3rd Workshop on PIV, Santa Barbara, CA, USA, UCSB University Press, pp. 545-550.
- Westerweel, J. Adrian, R.J., Eggels, J.G.M. Nieuwstadt, F.T.M. (1993): Measurements with particle image velocimetry of fully developed turbulent pipe flow at low Reynolds numbers. In: Applications of Laser Techniques in Fluid Mechanics, Eds.: Adrian et al., Berlin, Springer, pp. 476-499.
- Westerweel, J. Draat, A.A. van der Hoeven, J.G.Th. van Oord, J. (1996): "Measurements of fully-developed turbulent pipe flow with digital particle image velocimetry." Experiments in Fluids 20, pp. 165-177.